Magnetic-field-induced Fréedericksz transition and the dynamic response of nematic liquid-crystal films with a free surface

Shyu-Mou Chen and Ting-Chiang Hsieh
Institute of Electro-Optical Engineering, National Chiao Tung University, Hsinchu, Taiwan 30049, Republic of China

Ru-Pin Pan
Department of Electrophysics, National Chiao Tung University, Hsinchu, Taiwan 30049, Republic of China
(Received 13 April 1990; revised manuscript received 7 November 1990)

The Fréedericksz transition and the dynamic response of homeotropical liquid-crystal films with a free surface (FS) induced by a perpendicular dc magnetic field have been studied theoretically and experimentally for two nematic substances: 4′-*n*-pentyl-4-cyanobiphenyl (5CB) and 4′-*n*-octyl-4-cyanobiphenyl (8CB). For either one of these two materials, it is found that the critical magnetic field of these two nematic liquid-crystal (NLC) films with a free surface is equal to that of the NLC film with hard boundaries (HB) of the same thickness. This thus demonstrates a very strong orientational anchoring for 5CB and 8CB at the free surface. The intrinsic structures of FS samples are homeotropic, just as the HB ones are. For the dynamic response, the turn-off rates of FS samples are found to be about two times faster than those of the HB ones. This is interpreted with the backflow theory and the lack of positional anchoring on the free surface. Finally, a sensitive approach to determine the viscosity coefficients, γ_1 and η_c, of the NLC film is suggested.

I. INTRODUCTION

Surface effects of liquid crystals are important for both device applications and basic understanding of physical phenomena. The study of free-surface effects is even more interesting for understanding the anisotropy of molecular interactions. Previous studies have shown the existence of preferred molecular orientation at the free surface of nematic liquid crystals (NLC).[1,2] The strength of the free-surface-orientational anchoring and the effect of the lack of positional anchoring, however, remains to be clarified. Pan, Hsiung, and Shen[3] have reported the Fréedericksz transition[4] and relaxation response of 4′-*n*-pentyl-4-cyanobiphenyl (5CB) nematic liquid-crystal films with a free surface induced by a laser field. Since the molecular reorientation in the NLC film is restricted only in a small region about the size of the pump laser beam spot, the so-called "beam size effect" must be considered. The focused laser beam also induces other problems such as local thermal heating in the sample.

In this work, a dc magnetic field is used to induce molecular reorientation to avoid these problems. We study the critical transition magnetic field H_c, and the dynamic response time constants of NLC of 5CB and 8CB (4′-*n*-octyl-4-cyanobiphenyl) films with a free surface under the magnetic field. For comparison, these properties of similar films but with hard boundaries (i.e., NLC films sandwiched between glass substrates) are also studied.

In Sec. II, starting from the free energy of NLC films, we derive the critical field H_c for the Fréedericksz transition. We then use the theory of Ericksen and Leslie[5] to derive the turn-on and turn-off time constants of the NLC films, under a dc magnetic field, for small molecular orientational angle θ. We also show the differential relaxation time constant of a small variation $\Delta\theta$ around an equilibrium angle in a field H. In particular, we compare the backflow effect[6] on these time constants of free-surface (FS) samples and hard-boundary (HB) samples. In Sec. III, the experimental methods and the experimental results are presented. The comparison between the experimental and the theoretical results is discussed in Sec. IV. In Sec. V, we give a conclusion of this work and suggest a sensitive method to determine the viscosity coefficients, γ_1 and η_c, of the NLC by measuring the turn-off time constants of the HB and FS samples.

II. THEORY

A. The critical magnetic field for the Fréedericksz transition

For a homeotropically aligned NLC film with a free surface, the critical magnetic field H_c can be derived using the same approach as that used in Ref. 3 for the critical laser intensity. Let $\hat{\mathbf{z}}$ be the surface normal and θ be the molecular reorientational angle from $\hat{\mathbf{z}}$, the director $\hat{\mathbf{n}}$ and external magnetic field $\mathbf{H}$ applied parallel to the NLC film surface are expressed as $\hat{\mathbf{n}}=(\sin\theta(z),0,\cos\theta(z))$ and $\mathbf{H}=(H,0,0)$, respectively. The free-energy density F of the NLC film can be written as

$$F=\frac{1}{2}\left[K_{11}\sin^2\theta\left[\frac{\partial\theta}{\partial z}\right]^2+K_{33}\cos^2\theta\left[\frac{\partial\theta}{\partial z}\right]^2-\chi_a H^2\sin^2\theta\right], \tag{1}$$

where K_{11}, K_{33} are Frank elastic constants, and $\chi_a\equiv\chi_\parallel-\chi_\perp$, with $\chi_\parallel$ and $\chi_\perp$ being the diamagnetic suscep-

tibilities parallel and perpendicular to the director, respectively. Using the Euler–Lagrange equation to minimize the total free energy, we can get a simplified linear equation in the small-angle approximation,

$$K_{33}\frac{\partial^2\theta}{\partial z^2}+\chi_a H^2\theta=0 \ . \tag{2}$$

With the boundary condition $\theta(z=-d/2)=0$, where d is the film thickness. The solution is

$$\theta(z)=\theta_m \sin[q(z+d/2)] \ . \tag{3}$$

Substituting it into Eq. (2), we obtain the critical magnetic field

$$H_c=q(K_{33}/\chi_a)^{1/2} \ . \tag{4}$$

The q value in Eq. (4) is determined with another boundary condition of θ at $z=+d/2$.

For a HB sample, $\theta(z=+d/2)=0$, so $q=\pi/d$. For a FS sample, we have to consider the surface free energy at the free surface,[3,7] $F_s=\frac{1}{2}A\theta^2\delta(z-d/2)$, where A is the surface anchoring strength. Add it to the bulk free energy given in Eq. (1), Eq. (2) then becomes

$$K_{33}\frac{\partial^2\theta}{\partial z^2}+\chi_a H^2\theta=A\theta\delta(z-d/2) \ .$$

Substituting $\theta(z)$ of Eq. (3) into this equation and integrating it from $z=(d/2)^-$ to $z=(d/2)^+$, we get the boundary condition at $z=d/2$,[3]

$$-\frac{K_{33}}{A}=\frac{\tan(qd)}{qd} \ . \tag{5}$$

Thus the surface anchoring strength A determines the q value and then determines the critical magnetic field H_c. If A is very large, i.e., if the surface orientational anchoring is very strong, the H_c of the FS sample will be the same as that of the HB sample. Otherwise, the former must be smaller than the latter. On the other hand, the A value can be estimated from the measured H_c values of the FS and HB samples. A more detailed derivation for Eq. (5) but with both interfaces having same anchoring strength can be found in Ref. 8.

B. Dynamic response time constants

The dynamic behavior of the molecular reorientation in NLC films is complicated because its motion is coupled with the fluid flow. In this subsection, we first briefly review some results of Pieranski, Brochard, and Guyon,[9] where response time constants are derived from the simplified equations of motion, which are applicable for small reorientational angle θ only. We then derive the differential relaxation time constant τ_d for small change in angle $\Delta\theta$ about an equilibrium angle θ_∞ from the equations of motion without small-angle approximation.

If the external magnetic field H is changed abruptly from an initial field H_1 smaller than the critical field H_c to a field H larger than H_c, the liquid-crystal molecules will begin to rotate, and we define the dynamic exponential time constant at the beginning as the turn-on time constant τ_{on}. Similarly, if the magnetic field is changed from $H_2>H_c$ to $H<H_c$, the molecular orientation will relax to $\theta=0$. We define the exponential time constant at the end as the turn-off time constant τ_{off}. Following Pieranski *et al.*, we take τ_{on} to be positive and τ_{off} to be negative.

For small reorientation angle θ, the coupled equations of motion for the director $\hat{\mathbf{n}}=(\theta,0,1)$ and the flow velocity $\mathbf{v}=(v_x(z),0,0)$ can be written as[9]

$$K_{33}\frac{\partial^2\theta}{\partial z^2}+\chi_a H^2\theta=\gamma_1\frac{\partial\theta}{\partial t}+\alpha_2\frac{\partial v_x}{\partial z} \ , \tag{6a}$$

$$\frac{\partial}{\partial z}\left[\eta_c\frac{\partial v_x}{\partial z}+\alpha_2\frac{\partial\theta}{\partial t}\right]=0 \ , \tag{6b}$$

where $\eta_c\equiv\frac{1}{2}(\alpha_4+\alpha_5-\alpha_2)$, $\gamma_1\equiv\alpha_3-\alpha_2$, and $\alpha_1,\ldots,\alpha_6$ are the viscosity coefficients following the notations of Ref. 4.

For HB samples, these equations can be solved to satisfy the boundary conditions, $\theta=v_x=0$, at $z=\pm d/2$.[10] The time constant, $\tau_{HB}(H)$, can be written as[9]

$$\tau_{HB}^{-1}(H)=\frac{\chi_a}{\gamma_{1,HB}^*(h)}(H^2-H_c^2) \ , \tag{7a}$$

where $\gamma_{1,HB}^*(h)$ is an effective viscosity and is a function of $h=H/H_c$. For small fields ($h^2<5$), the relative variation of $\gamma_{1,HB}^*$ with h is negligible, and

$$\gamma_{1,HB}^*\cong(1-\tfrac{1}{6}\alpha_2^2/\gamma_1\eta_c)\gamma_1<\gamma_1 \ . \tag{7b}$$

At the free surface, although the orientational anchoring is very strong, the positional anchoring is lacking. The *effective* strong anchoring at the free surface for 5CB and 8CB samples *for the film thickness range in our work* will be demonstrated in the next section from the fact that the experimental results of H_c of FS samples are equal to that of HB ones of same thickness. Therefore, the boundary conditions for FS samples are

$$\theta=v_x=0 \quad \text{at } z=-d/2 \ ,$$

and (8)

$$\theta=\frac{\partial v_x}{\partial z}=0 \quad \text{at } z=+d/2 \ .$$

To satisfy these boundary conditions, we choose the trial solution for Eq. (6) as

$$\theta(z,t)=\theta_0\cos\left[\frac{\pi}{d}z\right]\exp(t/\tau) \ , \tag{9a}$$

$$v_x(z,t)=v_0\left[1+\sin\left[\frac{\pi}{d}z\right]\right]\exp(t/\tau) \ . \tag{9b}$$

We thus obtain a similar equation for the response time constant of FS samples, $\tau=\tau_{FS}(H)$,

$$\tau_{FS}^{-1}(H)=\frac{\chi_a}{\gamma_{1,FS}^*}(H^2-H_c^2) \ , \tag{10a}$$

where

$$\gamma_{1,FS}^*=(1-\alpha_2^2/\gamma_1\eta_c)\gamma_1 \ . \tag{10b}$$

The sign difference for τ_{on} and τ_{off} has been reflected in Eqs. (7a) and (10a).

If the applied magnetic field is turned off from an initial field larger than H_c, the zero-field turn-off rate $\tau^{-1}(0)$ can be deduced from Eqs. (7a) and (10a) to be

$$\tau^{-1}(0)=-(K_{33}/\gamma_1^*)(\pi^2/d^2) , \tag{11}$$

where $\gamma_1^*=\gamma_{1,\mathrm{HB}}^*$ or $\gamma_{1,\mathrm{FS}}^*$ for HB or FS samples, respectively.

We define the relaxation time constant for small variation in angle $\Delta\theta$ around the equilibrium angle θ in a magnetic field H as the differential time constant. The maximum reorientational angle θ_m of homeotropic NLC film under a magnetic field H is[10]

$$\theta_m^2=2(1-h^{-2})/(1+\eta) , \tag{12}$$

where $\eta\equiv(K_{11}/K_{33})-1$, e.g., $\theta_m>20°$ for $h=1.1$. In general, θ is not a small value. The simplified equations of motion for small angles are no longer valid. We must start from more general equations of motion to derive the differential time constant τ_d. These equations are[11]

$$\gamma_1\frac{\partial\theta}{\partial t}=[K_{33}+(K_{11}-K_{33})\sin^2\theta]\frac{\partial^2\theta}{\partial z^2}+\tfrac{1}{2}(K_{11}-K_{33})\sin(2\theta)\left[\frac{\partial\theta}{\partial z}\right]^2+\tfrac{1}{2}\chi_a H^2\sin(2\theta)+\tfrac{1}{2}[\gamma_1-\gamma_2\cos(2\theta)]\frac{\partial v_x}{\partial z} , \tag{13a}$$

and

$$\frac{\partial}{\partial z}\left[(\alpha_1\sin^2\theta\cos^2\theta-\tfrac{1}{2}\alpha_2\cos^2\theta+\tfrac{1}{2}\alpha_3\sin^2\theta+\tfrac{1}{2}\alpha_4+\tfrac{1}{2}\alpha_5\cos^2\theta+\tfrac{1}{2}\alpha_6\sin^2\theta)\frac{\partial v_x}{\partial z}+(\alpha_2\cos^2\theta-\alpha_3\sin^2\theta)\frac{\partial\theta}{\partial t}\right]=0 , \tag{13b}$$

where $\gamma_2=\alpha_3+\alpha_2$ (Ref. 4). If θ is small, these equations reduce to Eq. (6).

Again, using the boundary conditions, we can write the trial solutions of Eq. (13) for HB sample as[12]

$$\theta(z,t)=\theta_\infty(z)+\Delta\theta(z,t) , \tag{14a}$$

and

$$v_x(z,t)=v_m(t)[\sin(qz)-2z/d] , \tag{14b}$$

where $\theta_\infty(z)=\theta_m\cos(qz)$is the molecular reorientation at steady state, $\Delta\theta(z,t)=\phi_m(t)\cos(qz)$, and $q=\pi/d$.

In steady state, $\theta(z,t)=\theta_\infty(z)$, $\partial\theta/\partial t=0$, and $v_x(z,t)=0$, Eq. (13a) reduces to the static equation,

$$[K_{33}+(K_{11}-K_{33})\sin^2\theta_\infty]\frac{\partial^2\theta_\infty}{\partial z^2}+\tfrac{1}{2}(K_{11}-K_{33})\sin(2\theta_\infty)\left[\frac{\partial\theta_\infty}{\partial z}\right]^2+\tfrac{1}{2}\chi_a H^2\sin(2\theta_\infty)=0 . \tag{15}$$

Using the trial solutions and the static equation, Eq. (13) can be transformed into equations of the differential variations $\phi_m(t)$, and $v_m(t)$. Because ϕ_m is small, these equations can be linearized further by keeping only terms up to the first order in ϕ_m and v_m. Finally, the variable z can be eliminated by integrating these equations from $z=-d/2$ to $+d/2$ after Eq. (13a) is multiplied by $\cos(qz)$. These equations of motion then reduce to the form

$$\gamma_1\frac{\partial\phi_m}{\partial t}+\gamma_1\frac{1}{\tau_{d0}}\phi_m=\gamma_{\mathrm{HB}}qv_m , \tag{16a}$$

$$qv_m=-\frac{B}{A_{\mathrm{HB}}}\frac{\partial\phi_m}{\partial t} . \tag{16b}$$

Combining the last two equations, we obtain the differential time constant,

$$\tau_{d,\mathrm{HB}}=\left[1+\frac{B}{A_{\mathrm{HB}}}\frac{\gamma_{\mathrm{HB}}}{\gamma_1}\right]\tau_{d0} , \tag{17}$$

where τ_{d0} is the differential time constant without considering the backflow effect, and

$$\begin{aligned}
&\tau_{d0}=\gamma_1\{q^2[K_{33}+(K_{11}-K_{33})G_1]+\chi_a H^2G_2\}^{-1} ,\\
&\gamma_{\mathrm{HB}}=\tfrac{1}{2}(\gamma_1-\gamma_2)(1-8/\pi^2)+\gamma_2G_3 ,\\
&A_{\mathrm{HB}}=\eta_c+\alpha_1G_4+\gamma_2G_5+\alpha_1G_6+\gamma_2G_7 ,\\
&B=\alpha_2-\gamma_2G_5 ,\\
&G_1=\sum_{n=0}^{\infty}(-1)^n\frac{2n+3}{4(n+1)(2n+1)!}(2\theta_m)^{2(n+1)}p_n ,\\
&G_2=\sum_{n=0}^{\infty}(-1)^{n+1}\frac{2}{(2n)!}(2\theta_m)^{2n}p_n ,\\
&G_3=\sum_{n=0}^{\infty}(-1)^n\frac{1}{2(n+1)!}(2\theta_m)^{2(n+1)}\times\left[p_{n+1}-\frac{2}{\pi^2(n+2)p_n}\right] ,\\
&G_4=\sum_{n=0}^{\infty}(-1)^n\frac{2n+3}{8(2n+2)!}(4\theta_m)^{2(n+1)}p_n ,\\
&G_5=\sum_{n=0}^{\infty}(-1)^n\frac{2n+3}{2(2n+2)!}(2\theta_m)^{2(n+1)}p_n ,\\
&G_6=\frac{1}{2\pi^2}\sum_{n=0}^{\infty}(-1)^{n+1}\frac{1}{(2n+2)!}(4\theta_m)^{2(n+1)}p_n^{-1} ,\\
&G_7=\frac{2}{\pi^2}\sum_{n=0}^{\infty}(-1)^{n+1}\frac{1}{(2n+2)!}(2\theta_m)^{2(n+1)}p_n^{-1} ,
\end{aligned} \tag{18}$$

and

$$p_n=\frac{1}{2}\frac{3}{4}\frac{5}{6}\cdots\frac{2n+1}{2n+2} .$$

For FS samples, the following trial solutions are used for Eq. (13) to satisfy the boundary conditions:

$$\theta(z,t)=\theta_\infty(z)+\Delta\theta(z,t) , \tag{19a}$$

$$v_x(z,t)=v_m(t)[\sin(qz)+1] . \tag{19b}$$

Following the same procedure as for the HB case, we obtain the differential time constant of FS samples,

$$\tau_{d,\mathrm{FS}}=\left[1+\frac{B}{A_{\mathrm{FS}}}\frac{\gamma_{\mathrm{FS}}}{\gamma_1}\right]\tau_{\mathrm{d0}}\ , \tag{20}$$

where $A_{\mathrm{FS}}=\eta_c+\alpha_1 G_4+\gamma_2 G_5$, and $\gamma_{\mathrm{FS}}=\frac{1}{2}(\gamma_1+\gamma_2 G_2)$.

Equations (17) and (20) are consistent with τ_{off} at magnetic field H smaller than the critical field H_c.

C. The backflow effect

As shown in Eqs. (6) and (13), the molecular reorientations are coupled with the fluid flow. When a NLC sample is driven by external torques, the molecules are put into rotation. This rotation induces hydrodynamic motion, and this flow also affects the orientational motion.

We would like to compare theoretically the backflow effect on the differential time constant of HB and FS samples. To this end, the differential relaxation rates $(1/\tau_d)$ as a function of H^2 for HB and FS samples, and also for the case of neglecting the backflow effect, are calculated and shown in Fig. 1. These results are for 5CB film at 25 °C with thickness equal to 200 μm. The parameters used are $K_{11}=0.54\times10^{-6}$ dyn, $K_{33}=0.72\times10^{-6}$ dyn, $\chi_a=1.047$ cgs units,[13] $\gamma_1=0.806$ P, $\gamma_2=-0.894$ P, $\alpha_2=-0.8485$ P, $\alpha_3=-0.0432$ P, and $\eta_c=1.12$ P.[14] Equations (4) and (12) are used to determine H_c and θ_m.

The results are very interesting in two aspects. For $H<H_c$, the backflow effect on both the HB and FS samples is to reduce the effective viscosity and then to increase the relaxation rate. In particular, the turn-off time constant of FS samples is about four times shorter than that of HB samples. On the other hand, for $H>H_c$, the backflow effect on the HB sample can be neglected. It, however, causes the relaxation rate to increase when H is just above H_c for FS samples. As H is increased, this effect slowly diminishes and then reverses the influence on the effective viscosity. That is, the relaxation rate of the FS sample becomes slower than that of the HB sample. This is caused by the direction change of the backflow torque. Parodi has pointed out that the directions of the backflow torque for $\theta=0°$ and 90° are opposite.[15] As a result, it should change sign at a particular angle θ_m as the magnetic field H is gradually changed.

III. EXPERIMENTAL METHODS AND RESULTS

The 5CB and 8CB material used in this experiment was purchased from British Drug Houses, Inc. Their nematic phase ranges are 22.5–35.2 °C and 33.5–40.2 °C (Ref. 16), respectively. The preparation procedure of the samples has been reported elsewhere.[3]

For both HB and FS samples, the film thicknesses range from 125 to 300 μm. These are measured either mechanically with a probe pin[3] or interferometrically within an accuracy of about ±2 μm. A detailed description of these methods has been presented in a recent paper.[17]

The sample was mounted horizontally in an oven. The oven temperature was stabilized at 25.0±0.05 °C for 5CB samples and at 35.0±0.05 °C for 8CB samples. The dc magnetic field H is applied parallel to the NLC film surface. The molecular reorientation of the NLC film is probed by the optical birefringence technique: a He-Ne laser beam polarized at 45° to the magnetic field is normally incident to the NLC film. As the molecules rotate

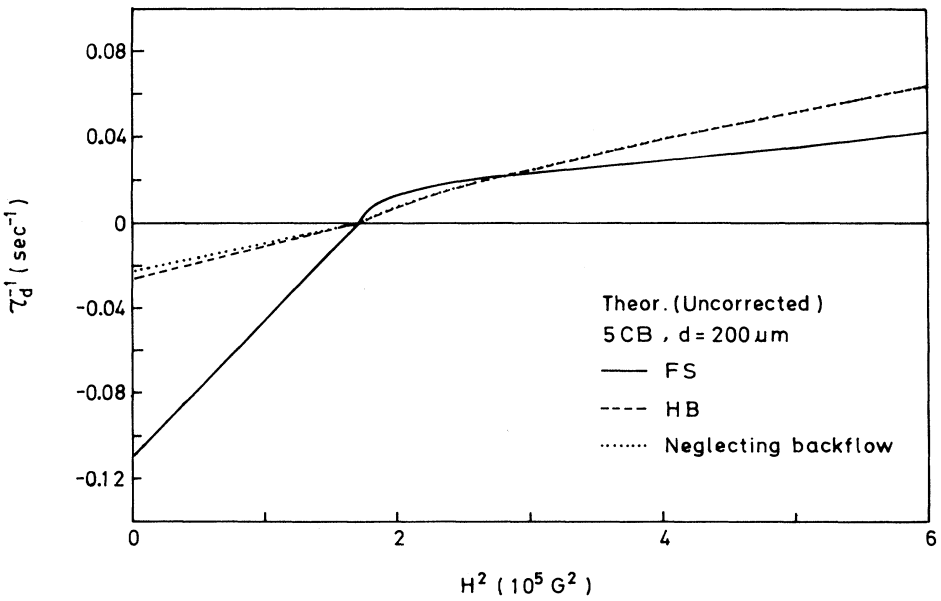

FIG. 1. The theoretical curves of the differential relaxation rate $(1/\tau_d)$ of a 200-μm-thick film vs the square of the magnetic field for a 5CB HB sample (dashed curve), FS sample (solid curve), and for the case of neglecting the backflow effect (dotted curve). Parameters from the literature are used.

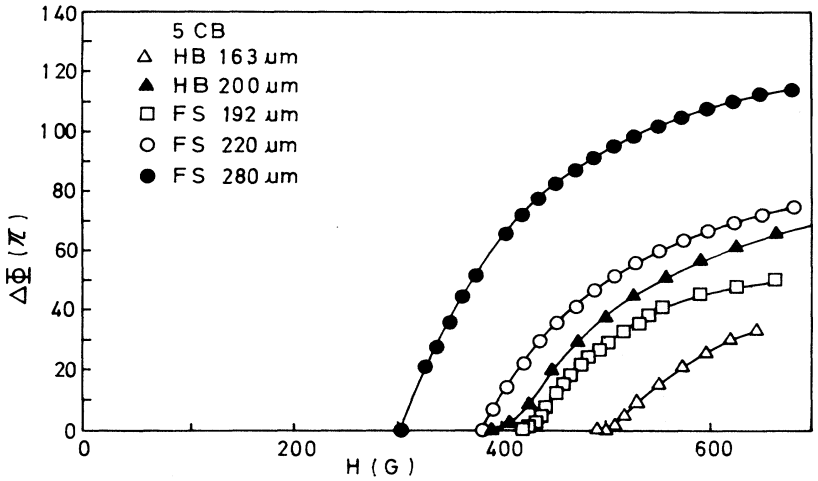

FIG. 2. Measured phase difference ($\Delta\Phi$) vs magnetic field H for several 5CB HB and FS samples with various film thicknesses.

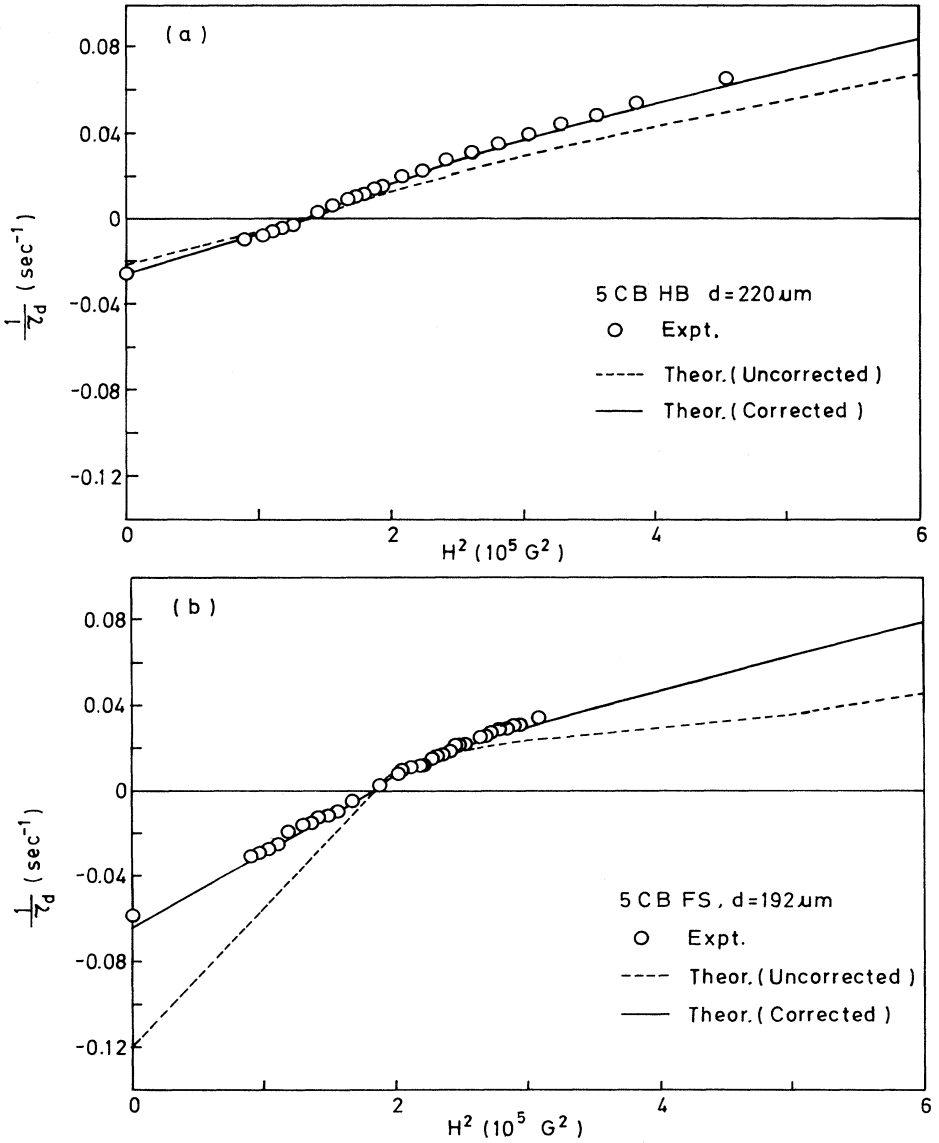

FIG. 3. Inverse of the differential time constant vs the square of magnetic field for (a) a 220-μm-thick 5CB HB sample, and (b) a 192-μm-thick 5CB FS sample. Open circles: experiment; dashed curves: theoretical, with viscosity coefficients from the literature; solid curves: theoretical, with corrected viscosity coefficients.

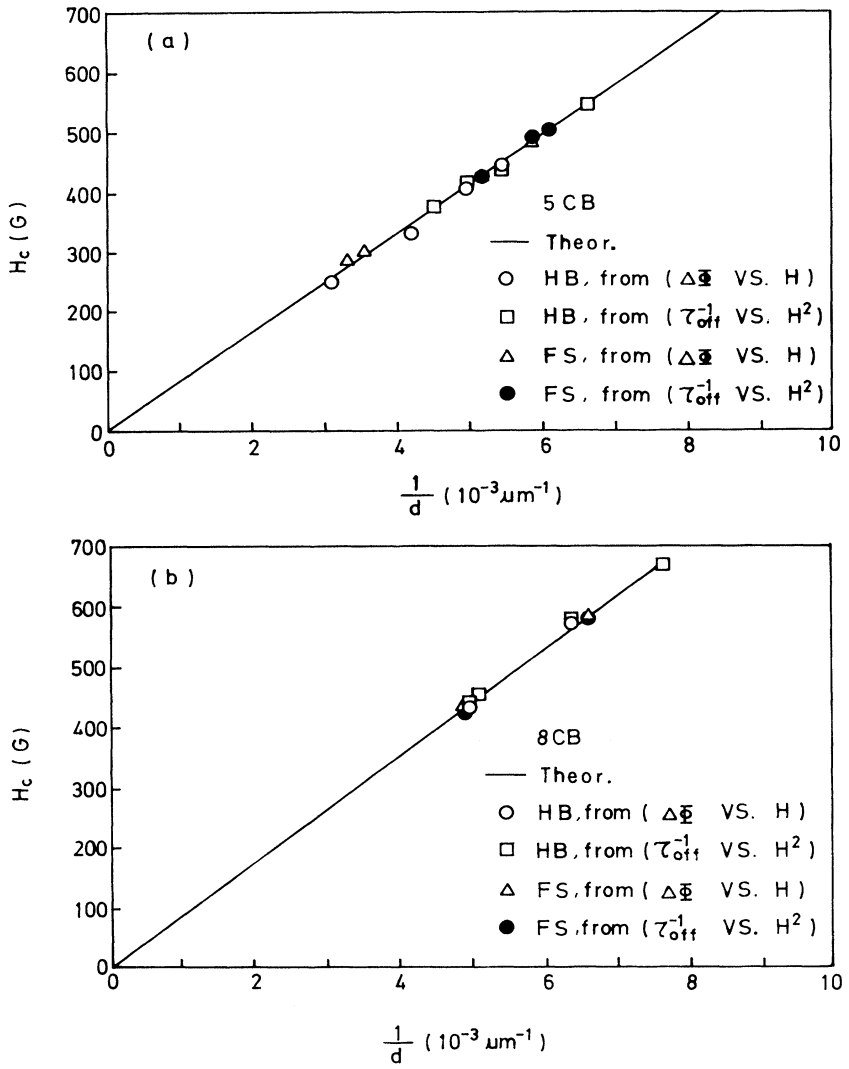

FIG. 4. Critical magnetic field H_c of (a) 5CB and (b) 8CB HB and FS samples vs the inverse of film thickness $1/d$.

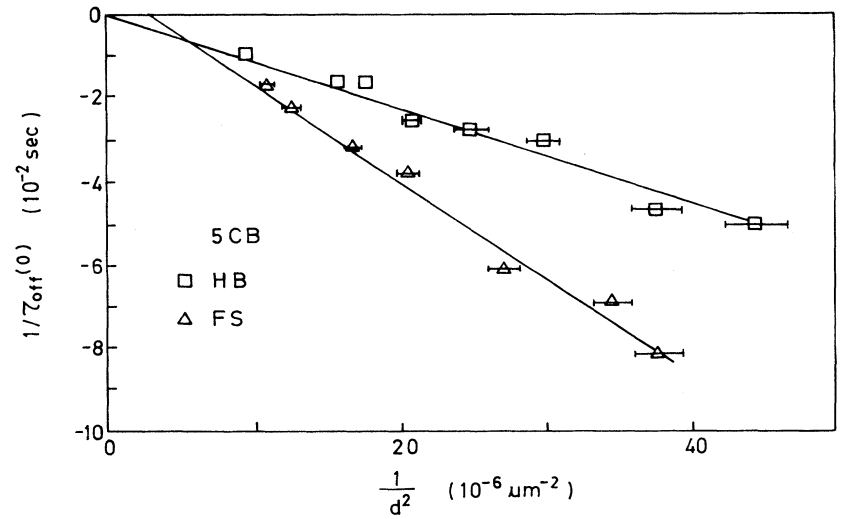

FIG. 5. The inverse of the turn-off time constant ($1/\tau_{\text{off}}$) obtained when the magnetic field is changed from $H > H_c$ to zero plotted as a function of $1/d^2$ of 5CB samples.

in the plane of **H** and the normal of the NLC film surface, the refractive index of the *e* ray is changed with the molecular orientational angle θ,[18]

$$n_{\text{eff}}=\left[\frac{\cos^2\theta}{n_0^2}+\frac{\sin^2\theta}{n_e^2}\right]^{-1/2} .$$

Thus, with an analyzer crossed with the polarizer, the output probe beam intensity I_0 is

$$I_0(t)=I_i\sin^2[\Delta\Phi(t)/2] ,$$

where I_i is the input probe intensity, $\Delta\Phi(t)$ is the phase difference between the *o* beam and *e* beam after the probe beam traversing the NLC film, i.e.,

$$\Delta\Phi(t)=\frac{2\pi}{\lambda}\int_{-d/2}^{+d/2}[n_{\text{eff}}(z)-n_0]dz .$$

Using the photodetector to sense the output intensity and a Y-T recorder to record the variation of I_0 with time, we can deduce the variation of the molecular reorientation angle θ with time when the magnetic field is changed.

The measured static phase difference $\Delta\Phi$ as a function of the magnetic field H for several 5CB HB and FS samples of various film thicknesses is shown in Fig. 2. The critical magnetic field H_c for each case can be identified clearly in the figure. From Eqs. (7a) and (10a), H_c can

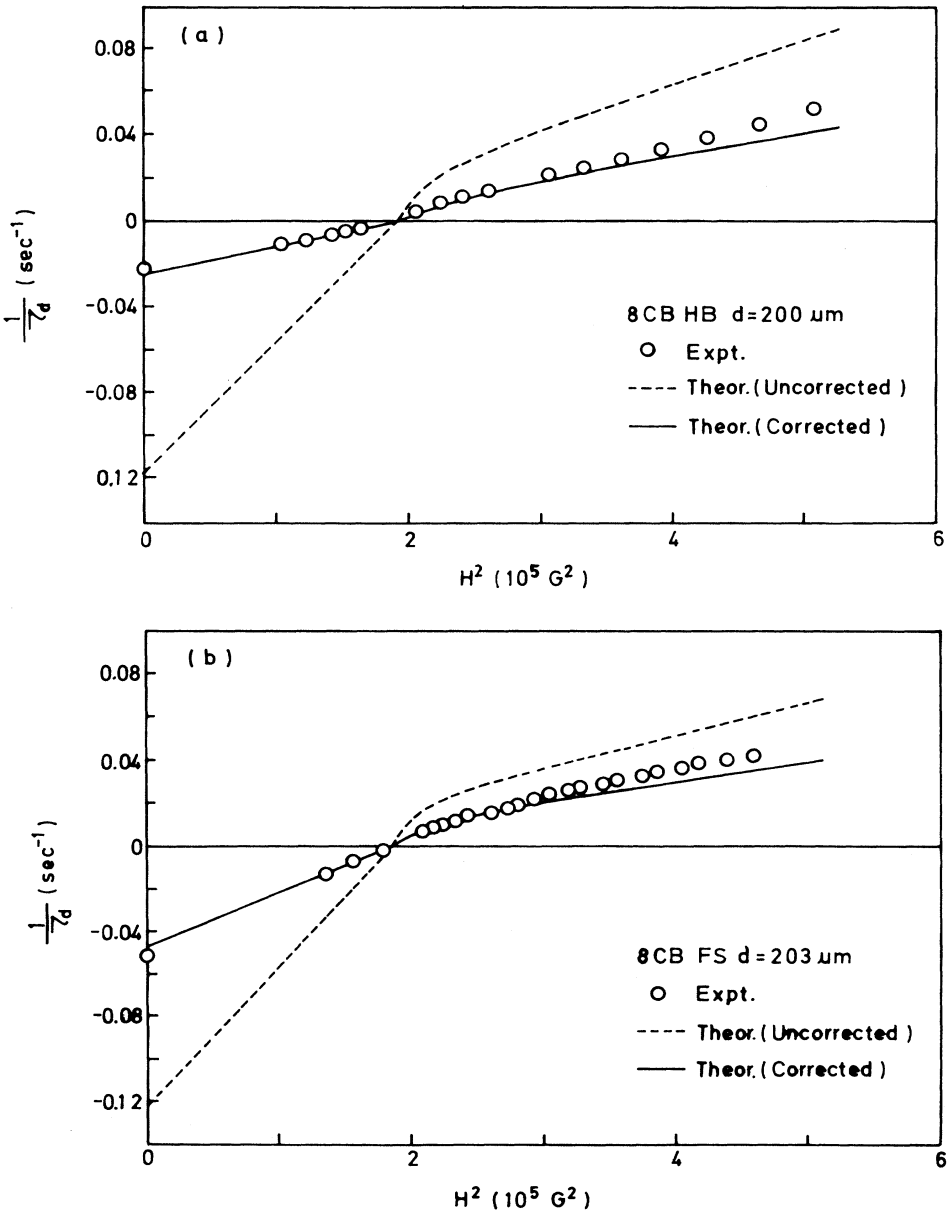

FIG. 6. The inverse of differential time constant vs the square of magnetic field for (a) a 200-μm-thick 8CB HB sample and (b) a 203-μm-thick 8CB FS sample. Open circles: experiment; dashed curves: theoretical, with viscosity coefficients of 8CB from the literature; solid curve: theoretical, with correlated viscosity coefficients.

also be obtained from the measurement of $1/\tau_{\rm off}$ as a function of H^2. Figures 3(a) and 3(b) show the variation of the relaxation rate $1/\tau_d$ of a 5CB HB and FS sample with respect to H^2. As the magnetic field is changed from $H_1 > H_c$ to $0 < H < H_c$, τ_d becomes $\tau_{\rm off}$ according to our definitions.

Using these two methods, the critical field H_c of HB and FS samples of various thicknesses is determined and is displayed in Fig. 4(a) for 5CB as a function of $1/d$. It is shown that the critical magnetic fields H_c of HB and FS samples of the same thickness are almost equal to each other within experimental accuracy. Similar results are obtained for 8CB samples, as shown in Fig. 4(b).

The variation of the zero-field turn-off rate $1/\tau_{\rm off}(0)$ with $1/d^2$ for 5CB HB and FS samples is shown in Fig. 5, from which we can see that the zero-field turn-off rate of FS samples is faster than that of HB samples by a factor of about 1.95 for the same thickness. This is consistent with the experimental result of Ref. 3, in which the molecular reorientation of the NLC film is induced by a laser light.

A set of measured differential relaxation rates as a function of H^2 for 5CB HB and FS samples is presented in Figs. 3(a) and 3(b), respectively. Similar results for 8CB are shown in Figs. 6(a) and 6(b).

In the range of $0 < H < H_c$, $\tau_{\rm off}$ is equal to τ_d, as mentioned above. From Figs. 3(a) and 3(b) and 6(a) and 6(b), one observes that $1/\tau_{\rm off}$ varies linearly with H^2, as predicted by the theory [see Eqs. 7(a) and 10(a)]. For 5CB, the slope of the curve of $1/\tau_{\rm off}$ versus H^2 of the FS sample is about 1.95 times larger than that of the HB sample. Thus the effective viscosity of the FS sample ($\gamma^*_{1,\rm FS}$) is about 1.95 times smaller than that of the HB sample ($\gamma^*_{1,\rm HB}$). For 8CB, the effective viscosity of the FS samples is 2.0 times smaller than that of the HB samples.

IV. COMPARISON BETWEEN EXPERIMENTAL RESULTS AND THEORY

Substituting the parameters for 5CB given in Sec. II, and $K_{33}=7.1\times10^{-7}$ dyn, $\chi_a=0.913\times10^{-7}$ cgs units[12] for 8CB at 35 °C, into Eq. (4), we obtain $H_c=8.234/d$ cgs units for 5CB and $H_c=8.76/d$ cgs units for 8CB. These are also plotted in Figs. 4(a) and 4(b) as the solid lines. Experimental results match the theoretical prediction almost exactly.

From the fact that the critical magnetic fields of HB and FS samples of the same thickness are almost equal to each other within the experimental accuracy, we can deduce that for 5CB and 8CB, the molecules near the free surface are homeotropically aligned and the orientational anchoring of the free surface is very strong, just as that for a hard boundary of a glass interface coated with dimethyl-*n*-octadecyl-3-amino propylmethoxysilyl-chloride (DMOAP). If we assume the experimental error is within 2%, using Eqs. (4) and (5) and with the values of 5CB parameters used above, we can estimate that the surface free-energy constant A is larger than 1.76×10^{-3} erg/cm^2.

We have shown that the linear relation of $1/\tau_{\rm off}$ and $1/\tau_d$ with H^2 in the range of $0 < H < H_c$ is in agreement with the theoretical prediction. However, the quantitative behavior of the former is very different from the latter. For example, in Sec. II we predicted that the turn-off relaxation rate of the FS sample is about four times faster than the HB case, but the experimental results are only 1.95 times faster. Figure 3(a) is the variation of $1/\tau_d$ with H^2 for a 5CB HB sample 220 μm in thickness. Comparing the measurement data (open circles) with the theoretical prediction (dashed curve) using the parameters listed in Sec. II, the difference is obvious. Similar results for a 5CB FS samples are shown in Fig. 3(b).

Results for a 8CB HB and FS samples are shown in Figs. 6(a) and 6(b), respectively. The discrepancy between experimental data (open circles) and theoretical prediction (dashed curve) with 8CB's viscosity coefficients obtained from Ref. 19 are even larger than the 5CB cases.

These discrepancies in $1/\tau_d$ can be caused by the uncertainties in the values of some of the parameters used according to the measurement error in the cited literature. The measurement principles of the previous workers are also different from ours. To resolve this problem, the parameters we need are obtained from our experimental results by comparing them with the theories. We first examine the measured zero-field turn-off time constants $\tau_{\rm off}(0)$ of HB and FS samples. From Fig. 5, the slopes of the lines of the $1/\tau_{\rm off}(0)$ versus $1/d^2$ for 5CB HB and FS samples through the origin are found to be -1.14×10^{-5} and -2.12×10^{-5} cm^2/s, respectively. According to Eq. (11), we can write

$$\frac{\pi^2 K_{33}}{[1-\alpha_2^2/(6\gamma_1\eta_c)]\gamma_1}=1.14\times10^{-5}\ , \tag{21a}$$

and

$$\frac{\pi^2 K_{33}}{[1-\alpha_2^2/(\gamma_1\eta_c)]\gamma_1}=2.12\times10^{-5}\ . \tag{21b}$$

From these equations we can obtain $\gamma_1\eta_c/\alpha_2^2=2.24$ cgs units. The experimental results of H_c, which is a function of K_{33}, are in good agreement with the calculated ones. We can thus assume the value of K_{33} is reliable. Because $\gamma_1=\alpha_3-\alpha_2$ and $|\alpha_3| \ll |\alpha_2|$, the influence of α_3 is small. We can further assume that α_3 does not need to

TABLE I. A comparison between our corrected viscosity coefficients from this work and the corresponding values obtained from the literature, for 5CB at 25 °C and for 8CB at 35 °C.

	5CB			8CB	
	Ref. 14	Ref. 19	This work	Ref. 19	This work
γ_1	0.806	0.93	0.68	0.48	0.801
γ_2	−0.894	−0.767	−0.767	−0.48	−0.886
α_2	−0.849	−0.93	−0.723	−0.48	−0.843
α_3[a]	−0.043	≅0	−0.043	≅0	−0.043
η_c	1.12	1.17	1.53	0.774	1.63

[a] α_3 is not adjusted in this work.

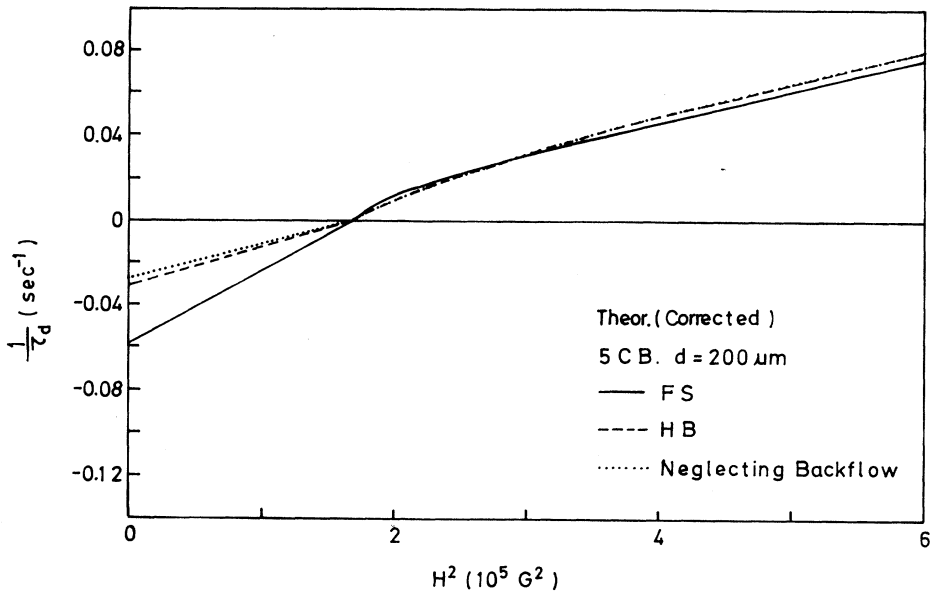

FIG. 7. The corrected theoretical curves of the differential relaxation rate ($1/\tau_d$) vs the square of the magnetic field for the 5CB HB sample (dashed curve), FS sample (solid curve), and for the case of neglecting the backflow effect (dotted curve). The films are 200 μm in thickness and the corrected viscosity coefficients are used.

be adjusted. After substituting the values of K_{33} and α_3 obtained from the literature (as used in Sec. II) into Eq. (21), we obtain $\gamma_1=0.68$ (thus $\alpha_2=-0.922$) and $\eta_c=1.53$ cgs units. These are consistent with the results of Pan, Hsiung, and Shen in Ref. 3.

Similarly, for 8CB, we obtain $\gamma_1=0.801$ and $\eta_c=1.63$ cgs units. These are not about twice as large as the corresponding values of Chmielewski in Ref. 19. The comparison between these corrected values and the corresponding values obtained from the literature are shown in Table I.

Using these corrected parameters, the calculated theoretical values of $1/\tau_d$ of 5CB films are shown as the solid curves in Figs. 3(a) and 3(b) for a 220-μm HB sample and a 192-μm FS sample, respectively. Comparing the corrected curves with the corresponding experimental data (open circles), the former is in excellent agreement with the latter for small H. It also matches better than the uncorrected curves (dashed curve) in the larger H range. Similar results for 8CB cases are shown in Figs. 6(a) and (b).

With these corrected viscosity coefficients, the theoretical differential relaxation rate as a function of H^2 both for 5CB HB and FS samples, and also for the case of neglecting the backflow effect, is calculated and shown in Fig. 7. In the range of $H>H_c$, there is still a crossover between the FS curve and the HB one as in Fig. 1, but the difference between the two curves is very small.

Finally, we note that the above approach for determining γ_1 and η_c can be done by using the slopes of the measured $1/\tau_d$ as a function of H^2 for $0<H<H_c$, for only one HB and one FS sample of any thickness.

V. DISCUSSIONS AND CONCLUSION

We have studied, theoretically and experimentally, the Fréedericksz transition and the dynamic response of two kinds of NLC (5CB and 8CB) films with a free surface induced by a perpendicular dc magnetic field.

The critical magnetic field H_c for either a 5CB or 8CB film with a free surface is equal to that for the film with hard boundaries of the same thickness. It thus demonstrates that the free surfaces of 5CB or 8CB films possess strong surface-induced orientational anchoring. Further, their intrinsic structures are homeotropic, just as DMOAP-coated HB samples.

For both 5CB and 8CB films, the measured turn-off rates of FS samples are about twice as fast as those of HB ones. This is due to the lack of the positional anchoring on the free surface, which can enhance the backflow effect and speed up the relaxation of the molecular reorientation. In the regime of $H>H_c$, the difference between the differential relaxation rate of the HB and the FS sample is very small.

The static and dynamic behaviors of 8CB samples are completely analogous to those of 5CB films. The relaxation time constant of the former is slightly larger than that of the latter. It is probably due to the longer length of 8CB molecules. This causes its viscosity to increase.

The viscosity constants γ_1 and η_c deduced from several laser-induced Fréedericksz transition experiments[3,20] always show some difference from the values found in the literature. These discrepancies have been interpreted as a

thermal heating effect or a laser beam size effect. From this work we would conclude that these effects are not the main reasons for the discrepancies. The turn-off time constant τ_{off} is very sensitive to the variation of γ_1 and η_c. In our work, γ_1 and η_c for 5CB are adjusted only by 20% and 5% from the values in Refs. 14 and 19, respectively. This causes the turn-off time constant τ_{off} of the FS sample to be doubled. Measuring the turn-off time constants of HB and FS samples thus provides a sensitive method to determine the viscosity coefficients γ_1 and η_c.

ACKNOWLEDGMENTS

This work was supported by the National Science Council of the Republic of China under Grant No. NSC78-0208-M009-16.

[1]J. Cognard, J. Adhes. **17**, 123 (1984).
[2]J. E. Proust, E. Perez, and L. Ter-Minassian-Saraga, Colloid Polym. Sci. **254**, 672 (1976); E. Perez, J. E. Proust, L. Ter-Minassian-Saraga, and E. Manev, *ibid.* **255**, 1003 (1977).
[3]R. P. Pan, H. Hsiung, and Y. R. Shen, Phys. Rev. A **36**, 5505 (1987).
[4]See, for example, P. G. de Gennes, *The Physics of Liquid Crystals* (Clarendon, Oxford, 1974), Chap. 5.
[5]S. Chandrasekhar, *Liquid Crystals* (Cambridge University Press, Cambridge, 1977), Chap. 3.
[6]F. Brochard, Mol. Cryst. Liq. Cryst. **23**, 51 (1973).
[7]H. L. Ong, Phys. Rev. A **28**, 2393 (1983).
[8]A. Rapini and M. Papoular, J. Phys. (Paris) Colloq. **30**, C4-54 (1969).
[9]P. Pieranski, F. Brochard, and E. Guyon, J. Phys. (Paris) **34**, 35 (1973).
[10]F. Brochard, P. Pieranski, and E. Guyon, Phys. Rev. Lett. **28**, 1681 (1972).
[11]C. Z. Van Doorn, J. Phys. (Paris) Colloq. **36**, C1-261 (1975).
[12]H. Hsiung, L. P. Shi, and Y. R. Shen, Phys. Rev. A **30**, 1453 (1984).
[13]N. V. Madhusudana and R. Pratibha, Mol. Cryst. Liq. Cryst. Lett. **89**, 249 (1982).
[14]K. Skarp, S. T. Lagerwall, and B. Stebler, Mol. Cryst. Liq. Cryst. **60**, 215 (1980).
[15]O. Parodi, J. Phys. (Paris) **31**, 581 (1970).
[16]D. A. Dunmur, M. R. Manterfield, W. H. Miller, and J. K. Dunleavy, Mol. Cryst. Liq. Cryst. **45**, 127 (1978).
[17]S. M. Chen, R. P. Pan, and C. L. Pan, Appl. Opt. **28**, 4969 (1989).
[18]M. Born and E. Wolf, *Principles of Optics* (Pergamon, Oxford, 1980), Chap. 14.
[19]A. G. Chmielewski, Mol. Cryst. Liq. Cryst. **132**, 339 (1986).
[20]S. D. Durbin, Ph.D. thesis, University of California, Berkeley, 1984.